Taylor & Francis
Taylor & Francis Group

Remote Sensing Letters

ISSN: 2150-704X (Print) 2150-7058 (Online) Journal homepage: www.tandfonline.com/journals/trsl20

Fast computation of digital terrain model anomalies based on LiDAR data for geoglyph detection in the Amazon

Fabien H. Wagner, Vinícius Peripato, Renato Kipnis, Sara L. Werdesheim, Ricardo Dalagnol, Luiz E.O.C. Aragão & Mayumi C. M. Hirye

REMOTE SENSING LETTERS
2022, VOL. 13, NO. 9, 935–945
https://doi.org/10.1080/2150704X.2022.2109942

Taylor & Francis
Taylor & Francis Group

OPEN ACCESS Check for updates

Fast computation of digital terrain model anomalies based on LiDAR data for geoglyph detection in the Amazon

Fabien H. Wagner[a,b], Vinícius Peripato[c], Renato Kipnis[d], Sara L. Werdesheim[e], Ricardo Dalagnol[a,b,f], Luiz E.O.C. Aragão[c] and Mayumi C. M. Hirye[g]

[a]Institute of the Environment and Sustainability, University of California, Los Angeles, CA, USA; [b]NASA-Jet Propulsion Laboratory, California Institute of Technology, Pasadena, CA, USA; [c]Remote Sensing Division, National Institute for Space Research—INPE, São José dos Campos, Brazil; [d]Archaeology Department, Scientia Consultoria Científica, São Paulo, Brazil; [e]Services, Science, Environmental Planning & Management, Worley, São Paulo, Brazil; [f]Department of Geography, School of Environment Education and Development, University of Manchester, Manchester, UK; [g]Quapá Lab, Faculty of Architecture and Urbanism, University of São Paulo—USP, São Paulo, Brasil

ABSTRACT
The detection of pre-Colombian geoglyphs, geometric structures outlined by trenches or walls, from airborne LiDAR data is usually made by visual observation of the variation in elevation and commonly using additional hillshading. Depending on the area covered by LiDAR to inspect and the variation in elevation, this method can be time consuming and inaccurate as it required to constantly adjust the contrasts of the elevation image or the parameter of the hillshading function, and the user can miss some important archaeological features. Here, we present a method to enhance the anomaly of the terrain without using focal operations to normalize the elevation of each pixel in relation to its neighbours. An example is given for two areas covered by LiDAR and containing geoglyphs under the forest cover in the Amazon and with a synthetic LiDAR footprint over a simulated dense forested area containing four geoglyphs with different shapes and height/depth characteristics. The normalization enables to remove the influence of the landscape mean elevation, to highlight the fine anomaly of the terrain. The produced equalized images enable a fast visual assessment of relief anomaly and of the presence of geoglyphs in large LiDAR datasets of hundreds or thousands of LAS files.

ARTICLE HISTORY
Received 17 April 2022
Accepted 31 July 2022

KEYWORDS
LiDAR; elevation model; geoglyphs detections; archeology

1. Introduction

In the last decades, Amazonian rainforests' pristine wildernesses has been challenged by the discovery of numerous geoglyphs, which are human-built earthworks, geometric structures outlined by trenches or walls of 1–7 m deep (Mann 2008). The geoglyphs are shaped like circles, diamonds, hexagons and interlocking rectangles, and their diameter can range from 100 to 350 m (Mann 2008). Only in the Brazilian state of Acre, over 450 pre-Columbian (pre-AD 1492) geoglyphs have been identified, occupying 13,000 km^2 (Watling et al. 2017).

CONTACT Fabien H. Wagner fhwagner@ucla.edu Institute of the Environmentand Sustainability, University of California, Los Angeles, CA 90095, USA

Furthermore, pre-Colombian cultures have also built other large structure such as mound villages, raised fields and fortification that has a positive anomaly in the relief (De Souza et al. 2019; Iriarte et al. 2020).

These earthworks are mainly found because of deforestation, when these large structures, once covered by dense forests, appear in the pastures. Because of the forest cover, a lot of these structures remain undiscovered. The light detection and ranging (LiDAR) technology enables to make very high resolution digital terrain model (DTM) to detect earthen or masonry archaeological features that is generally time-consuming, expensive and often impossible in remote tropical regions (Iriarte et al. 2020), even below dense tropical forest canopy, that could enable to map an expected large number of yet undiscovered geoglyphs. Currently, numerous scientific programmes are using these technologies such as in Brazil, the programme 'Improving Biomass Estimation Methods for the Amazon' EBA (EBA 2016) or The Sustainable-Landscapes program (Embrapa 2016), and it has become increasingly common to have LiDAR coverage of several hundred or thousands of km^2 covering intact Amazon forest.

For instance, no automated methods exist to find these geoglyphs and each image has to be visually interpreted in order to detect these small changes in the landscape elevation. This is relatively easy for deforested area, generally pasture are made in flat area, but more challenging under forest where less LiDAR points reach the ground or when the region have small hills. The most common workflow include the computation of the DTM from the LiDAR point cloud. Then, an interpreter makes the visual detection of small variation of relief directly in the elevation from the DTM by creating a shaded relief image, also called hillshade (Iriarte et al. 2020; Mestre et al. 2020; Henry, Shields, and Kidder 2019; Canuto et al. 2018; Stenborg, Schaan, and Figueiredo 2018; Fisher et al. 2017; Khan, Aragão, and Iriarte 2017; Evans et al. 2013; Chase et al. 2012).

The hillshade technique is suitable for a few LiDAR flight lines to inspect. However, depending on the area covered by LiDAR to inspect and the variation in elevation, this method can be inaccurate as the user can miss some important archaeological structures, masked by larger scale variation in elevation. Several visualizations for DTM exist to enhance archaeological features. For example, the Relief Visualization Toolbox (RVT) (Kokalj and Somrak 2019; Zakšek, Oštir, and Kokalj 2011) proposed ten methods proven to be effective for identification of small scale features in DTM, such as hillshading, simple local relief model (Hesse 2010) or Sky-View Factor (SVF) (Kokalj, Zakšek, and Oštir 2011) among others. Many more visualizations have been described, such as subtracting two DTMs with different resolution (Doneus and Briese 2006), and comparison on the methods are given (Bennett et al. 2012; Challis, Forlin, and Kincey 2011; Canuto et al. 2018). For slight depression, such as the geoglyphs, it is recommended to use Simple Local Relief Model (SLRM), which is the spatial anomaly in elevation (Canuto et al. 2018; Kokalj and Somrak 2019; Zakšek, Oštir, and Kokalj 2011; Hesse 2010).

The computation of spatial anomaly in elevation in order to remove the influence of the main elevation in the image contrasts often made the use of the focal statistics. The first step consists in computing the DTM at a high resolution and the mean elevation of the DTM in a square moving window of a defined size larger than the DTM spatial resolution. In a second step, the mean elevation is subtracted from the DTM to compute the anomaly (Doneus and Briese 2006). The main disadvantage of this methods is that it required to use a focal operation, that is computationally intensive, after the production of the DTM.

Here, we present a methodology to compute and enhance the elevation anomalies of terrain surface using DTMs at different spatial resolution obtained with the LiDAR LAS files (.las or.laz containing LiDAR point cloud) and without using focal operations. The method is designed to normalize the elevation of each pixel in relation to its neighbours and to remove the influence of the main elevation in the image contrast. Our methodology is based on the subtraction of DTMs with different resolution, such as by Doneus and Briese (2006), that also gives very similar results than (simple) Local Relief Model (Hesse 2010). Additionally, it gives a normalized image that provide sufficient information and a pleasant visualization to efficiently detect geoglyphs in few seconds, to ease the application on large sets of LiDAR point-cloud files. It takes advantage of open source software R (R Core Team 2020) and of a recent R package the lidR package to speed up the DTMs' computation for the LAS files (Roussel and Auty 2020). The method R code is available at https://doi.org/10.5281/zenodo.5087619

2. Materials and methods

2.1. LiDAR data

The dataset is constituted of discrete-return LiDAR data acquired for the Sustainable Landscapes Brazil project (Embrapa 2016) across several forested regions of Brazil during 2014 and 2018 using a 'LaserScan Optech Orion M300' and a 'LaserScan Optech ALTM 3100' scanning systens onboard an airplane at an average flight altitude of 900 m and 750 m, respectively. Multiple LiDAR returns were recorded with a minimum point density of 4 points per m^2. It is currently one of the largest dataset of high-resolution airborne LiDAR in the Amazon forests with the programme 'Improving Biomass Estimation Methods for the Amazon' EBA (EBA 2016). To illustrate our method, we used two LAS files from this dataset. In the figures, the coordinates have been modified to not reveal the exact locations of the geoglyphs. Additionally, in order to show the enhancement of the small variations in elevation provided by our method, three point-cloud datasets (.las files) of similar characteristics as the original LiDAR data were simulated for a fake landscape of two hills containing four geoglyphs, two walls on the left (a square and a circle) and two trenches (a circle and a square). To simulate the noise of DTM below forest, a positive noise generated from a Gamma distribution of shape parameter of 1 and scaled between 0 and 3 was added to the elevation value, for a random selection of 50% of the DTM pixels. We generated three LAS files, one with walls of +2 m and trenches of −3 m, one with walls of +1 m and trenches of −1.5 m and the last one with walls of +0.25 m and trenches of −0.50 m.

2.2. DTM anomaly computation and storage

To detect the characteristics subtle variations in elevation of the geoglyphs, the first step was to compute the DTM at 1 m spatial resolution. The LiDAR point cloud was processed into DTM with 1 m $\times$ 1 m cell size using the function grid_terrain from the lidR R packages (Roussel and Auty 2020). Specifically, in this function, the triangular irregular network algorithm (TIN) is used because this is the fastest interpolation techniques. In a second step, a DTM at a larger spatial resolution, in our case cell sizes of 4 $\times$ 4 m, is computed using the same the function grid_terrain. However, here, another algorithm of interpolation called inverse distance weighting (IDW) is used. This algorithm provides a higher quality mean elevation DTM. In the IDW algorithm were used a parameter *p* of zero (no decrease in weight with distance) and a parameter *k* of 2000 (number of *k*-nearest neighbours to compute the DTM). In a third step, the 4 m spatial resolution DTM is disaggregated to 1 m spatial resolution and subtracted to the DTM at 1 m resolution to obtain the elevation anomaly. The value of anomaly above 1.5 m or below −1.5 m is set to the value 1.5 and −1.5, respectively. In a last step, for storage on the disk and visualization in a geographic information system (GIS) program without any further adjustment, the elevation anomalies are normalized between 0 and 254 and saved as 8 bits unsigned integers. For one LAS file, the computation and storage of the anomaly takes 5.0 seconds on a computer with a processor Intel i9 with 6 cores (12 threads) and 64 Gb of RAM, and it can be further parallelized. The model R code to compute DTM Anomaly for one .las tile or for several .las tiles (running in parallel) is available at https://doi.org/10.5281/zenodo.5087619. To compare our results visually with the most common method used to detect the geoglyphs, the elevation hillshade, the hillshade was computed on the DTM at 1 m spatial resolution for both original .las files with the function sphere_shade of the rayshader R package, using a sun angle of 315° and a ratio between the *x* and *y* spacing and the *z* axis (zscale) of 0.1 (Morgan-Wall 2020). The hillshade with different angles and *zcale* were also computed on the simulated .las files to show how critical is the choice of hillshade parameters for geoglyph visualizations. Finally, our results were compared to five other methods for digital elevation model visualizations from the Relief Visualization Toolbox – RVT (Kokalj and Somrak 2019; Zakšek, Oštir, and Kokalj 2011) with the default parameters found in the RVT QGIS plugin version 0.8.0 : hillshade from multiple directions (16 directions, sun elevation of 35°, directions 1, 6 and 12 were used to compose the RGB image), negative and positive openess, sky-view factor (search radius 10 pixels, number of search direction: 16) and simple local relief model (radius for trend assessment: 20 pixels).

3. Results

The computation of the elevation anomaly enhanced the visibility of small variations in elevation (Figure 1). In the elevation image, Figure 1(a), the contemporary roads and the main details of the geoglyph can be distinguished but are not very sharp. With the correction from mean elevation Figure 1(c), all secondary road appears now, and it can be clearly observed that the geoglyphs are a squared ditch surrounded by a wall and a wall with rectangular shape. Note that these geoglyphs are actually covered by dense forest. The squared geoglyph has shown particularly large features, the trench and the wall are both larger than 3–4 m and the difference between the lowest point of the ditch and the high point on the wall can reach 1.5 m. The rectanguler geoglyph has shown smaller features, with less than 50 cm between the highest point on the wall and the surrounding area, with but is also entirely visible. The method enables to effectively normalize the landscape elevation with some exception near the rivers and their borders, where the changes in elevation are more pronounced. In the hillshade representation of elevation, Figure 1(e), the squared geoglyph is also visible but not entirely. Some details that are aligned with the sun angle use to compute hill shade simply disappear, such as

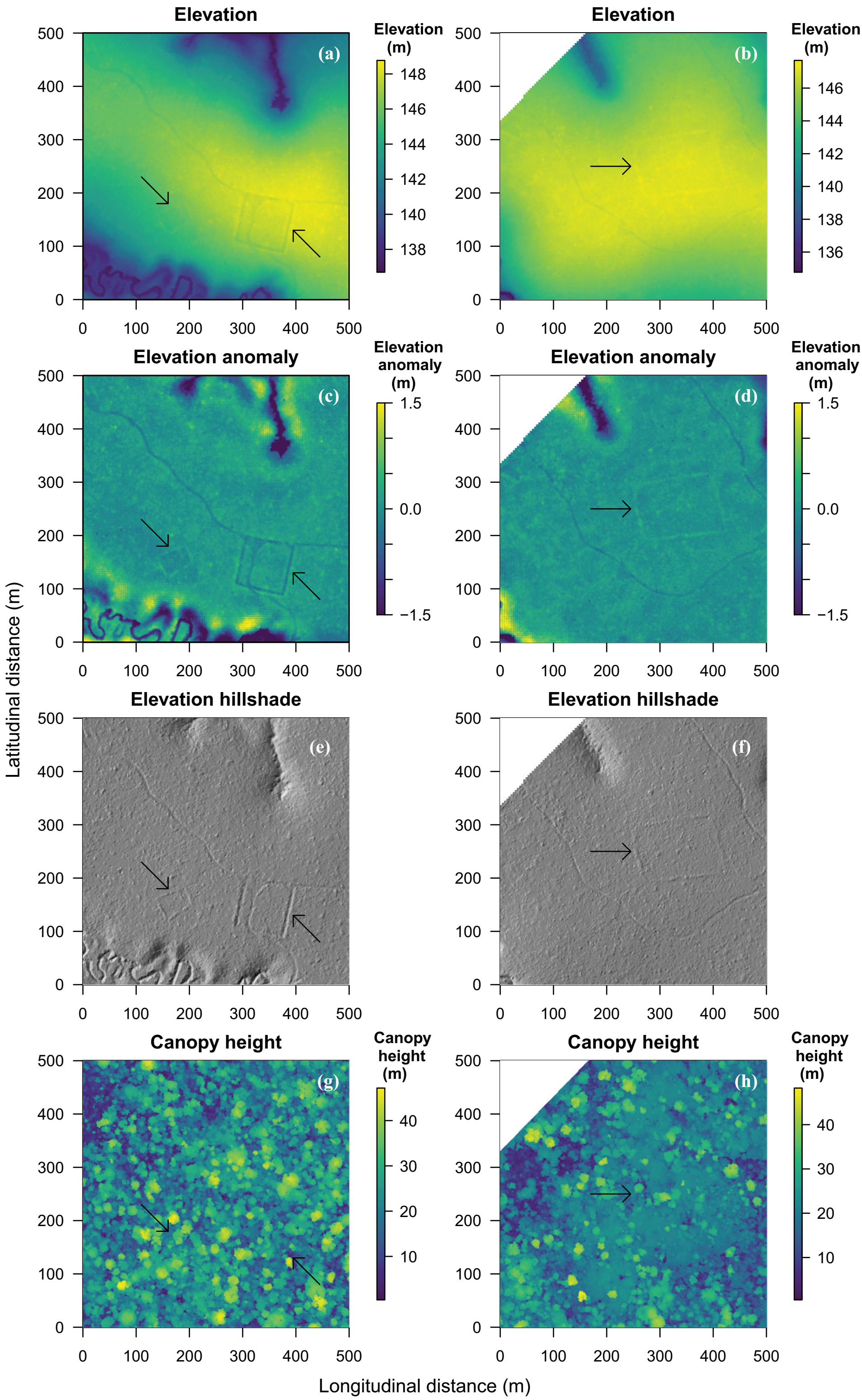

Figure 1. Example of elevation data, the corresponding elevation anomaly (our method), hillshade representation and canopy height for two .las tiles acquired over a dense Amazon forest (a-c-e-g and b-d-f-h, respectively). An anomaly value near 1 indicates a positive elevation anomaly (wall), near −1

a part of the road on the top left image. In the hillshade representation, Figure 1(e), the geoglyph cannot be clearly seen or interpreted as the trench or wall, such as possible with our method (Figure 1(c)).

The visualization of geoglyph with small variation in elevation (Figure 1(b,d and f)) is enhanced with our method. Without correcting for the elevation, Figure 1(b), the geoglyph is slightly visible but is easy to miss by the user. The contrast could be adjusted but this will impact the time of analysis of each image, as for example, here, the complete dataset is constituted of more than hundreds of LAS images like this one. Our method visualization provides better details of the structure (Figure 1(d)). The rectangular wall is 0.5–1 m in height, 4–6 m width and totally covered by dense tropical forest. The geoglyph in Figure 1(d) is easy to see, as geometric features are unexpected and draw visual attention. The user can really make a fast evaluation of the presence of geoglyphs in the images, in only a few seconds. Using hillshading for visualization on these smaller structures is problematic (Figure 1(f)); the rectangular wall needs more attention to be seen and we cannot determine visually if this is a trench or a wall.

Computing the anomaly using our method or using hillshading with different sun angles and zscale parameters on a simulated landscape with geoglyphs of the smallest height and depth (+0.25 m and −0.5 m) enables to compare the visualizations (Figure 2). In Figure 2(a), we can observe that our method detailed entirely the geometric forms. It is also easy to determine if the relief of the geoglyph is negative or positive only with the colour of the anomaly. One limitation however is the enhancement of anomaly near pronounced inversion of elevation (such as a river in the real world) and sometime near borders. Hillshade also provide in most of the case a visualization, but depending on the sun angle setting, some features of the geoglyphs disappeared, both on the squared and circular geoglyphs (Figure 2(c,e)). The hillshade image also shows large variation of contrast with elevation (Figure 2(c–f)) that rendered the image more complex to look as it still contains information of the main elevation of the landscape. For the computation of hillshade at a fixed sun angle, the zscale needs also to be adjusted (Figure 2(b,d and f)). With a too high zscale value (Figure 2(b)), the geoglyphs are not any more visible and for low value (Figure 2(d,f)), the image became very noisy, and need more effort to visualize in comparison to our method.

Comparing our result (Figure 3(a)) to the methods for digital elevation model visualization provided by the RVT Toolbox (Kokalj and Somrak 2019; Zakšek, Oštir, and Kokalj 2011) with the defaults parameters (Figure 3(b–f)), several observations can be made. First, hillshade from multiple directions gives a good enhancement of the geoglyph feature (Figure 3(b)); however, it has the same limitations that the standard hillshade, which are the fading of some features depending on the directions that have been chosen for the sun angles and some difficulties to determine if the geoglyphs are positive or negative in the landscape. Second, the negative openess enhances only the borders of the geoglyphs

a negative anomaly (trench) and 0 indicates no anomaly. Geoglyph locations are indicated by an arrow. Hillshade are computed with a sun angle of 315° and a zscale of 0.1. In the area covered by the first image (a-c-e-g), a rectangular geoglyph of 50 m constituted by a wall is visible on the bottom left side and the trench of a squared geoglyph of 100 m on the bottom right side. In the area covered by the second image (b-d-f-h), a rectangular geoglyph of 150 m constituted of a wall is visible on the right side. All the geoglyphs are under a dense amazonian forest cover (g-h) and the other structures visible in the images are contemporary roads and river beds.

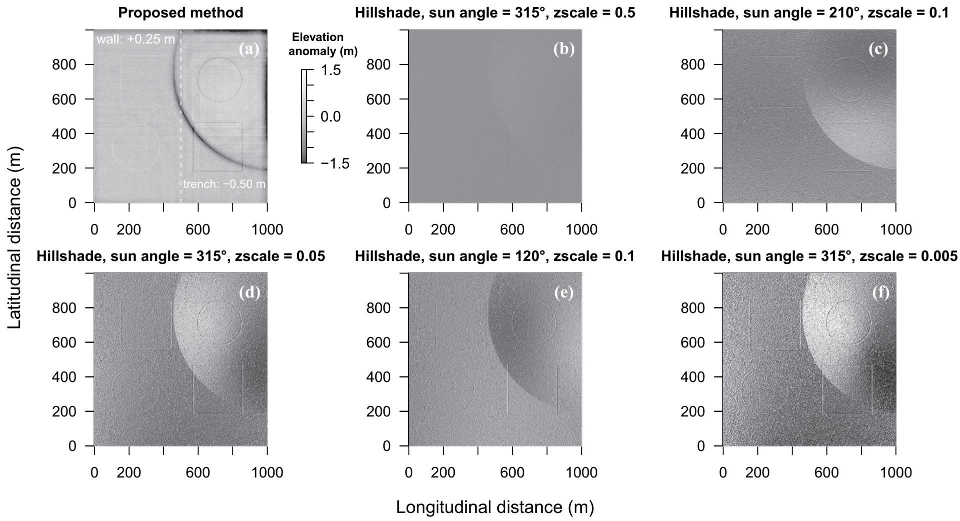

Figure 2. Example elevation anomaly computed with our method for a simulated landscape of two small hills containing four geoglyphs, two trenches of 0.5 m depth (a circle and a square) and two walls of 0.25 m height (a circle and a square) (a). An anomaly value near 1 indicates a positive elevation anomaly, such as a wall, a value near −1 a negative anomaly such as a trench and a value near 0 indicates no anomaly. Colors have been set to grayscale to compare with hillshade. Hillshade computed on the same elevation data that in (a) but with different parameters of sun angle and zscale factors (b-f).

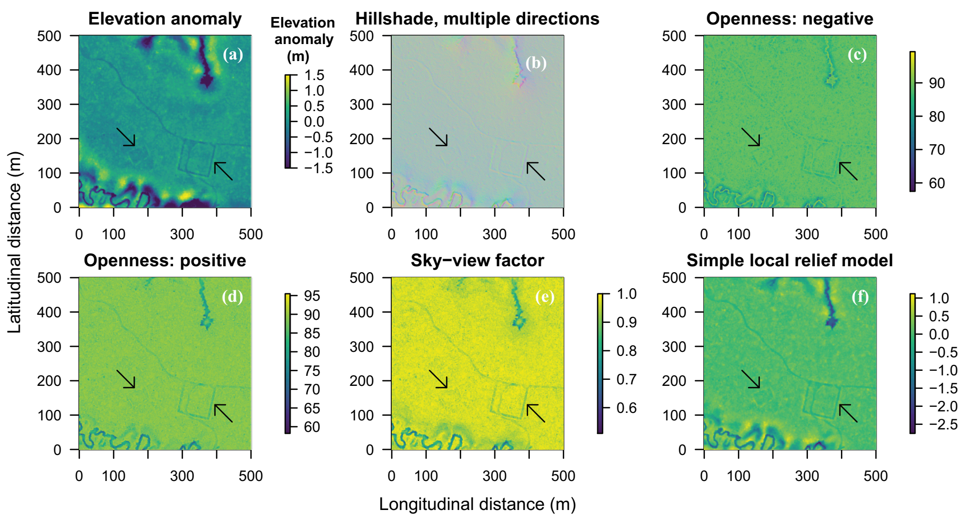

Figure 3. Example elevation anomaly computed with our method and five other methods for digital elevation model visualizations from Relief Visualization Toolbox – RVT (Kokalj and Somrak 2019; Zakšek, Oštir, and Kokalj 2011), a default standard in archaeology. The visualizations were all computed from the digital elevation model containing the two geoglyphs, a squared trenches and a rectangular walls. Elevation anomaly with our method (a), hillshade from multiple directions (b), negative openess (c), positive openess (d) sky-view factor (e) and simple local relief model (f).

(Figure 3(c)), where elevation in changing on same distance and the colour inside the trench or the roads is the same as outside. This renders the geoglyph a bit more difficult to interpret and the size of trench and wall widths are not anymore measurable. With positive openess (Figure 3(c)), the rectangular geoglyph is almost not visible anymore, while the squared geoglyph has a good visualization. The sky-view factor result (Figure 3(e)) is very similar to the positive openess, with a rectangular geoglyph that is not visible anymore. The small details on the roads and the geoglyphs also appear less smooth that with our method. Finally, Simple local relief model (SLRM) gives similar results like our method, as they are computed almost identically. However, the SLRM does not return a normalized results that could impede the visualization if there were large variations in elevation, and would not give an homogeneous visualization when opening several neighbouring SLRMs in a GIS, such as our method provides. And, more importantly, the SLRM function simply does not work with missing values in digital terrain model computed from a LAS file, which is common, and additional operations to remove missing values or to clip the DTM would be needed to compute the SLRM. The method for the RVT Toolbox is better than our method for the visualization of steep slope and large inversion of slope such as river beds, which appeared saturated in our method visualization due to the normalization.

4. Discussion

Here, we present a fast method to obtain elevation anomaly from LiDAR point-cloud data. It uses only the function to compute DTM from the lidR R packages (Roussel and Auty 2020) and does not need additional focal operation on the DTM. It is originally designed to detect geoglyphs, which are geometric structures outlined by slight increase or depression in elevation. It enables a fast visual assessment on the best visualization (elevation anomaly) for slight variations in elevation (Canuto et al. 2018). The proposed method, such as previously observed by simple local relief model (Hesse 2010) or even more similar DTMs subtraction methods (Doneus and Briese 2006), allow to visualize extremely shallow relief features, by confining the colour-coding to narrow values. The user does not have to make additional adjustment of the image contrast when importing the raster in a GIS program as the elevation anomaly raster is already scaled between 0 and 255 when saved. That is, it provides an elevation anomaly image in which the user can detect geoglyphs in a few seconds, enabling fast screening of large LiDAR datasets. Our method does not intend to replace visualization softwares like Relief Visualization Toolbox (RVT) (Kokalj and Somrak 2019; Zakšek, Oštir, and Kokalj 2011) that integrate a similar function called simple local relief model (Hesse 2010), but to provide, in the same time that the DTM is computed from the point cloud, elevation anomaly images that can be used directly in a GIS software without any supplementary manipulation for detecting the geoglyph presence. After detections, more refinement of the structure could benefit from the diverse visualizations offered by RVT. After the detections with our method, the user will work only with the few . las file where geoglyphs have been detected and will have more time to extract the maximum information from the point cloud or the DTM with multiple visualization methods (Challis, Forlin, and Kincey 2011; Bennett et al. 2012; Canuto et al. 2018; Kokalj and Somrak 2019; Zakšek, Oštir, and Kokalj 2011). For instance elevation, anomaly visualization of the LiDAR DTM of the Amazon geoglyphs is not common. This is likely because researchers on geoglyphs are used to the hillshading methods, because the size of the area to inspect enables a fine observation of the entire dataset and because most of them are outside the forest with dense pulses return. However, looking at archaeological structure below tropical forest is way more challenging as a mean of less than 10% of the LiDAR pulses reach the ground with sufficient energy to produce a detectable return (Mestre et al. 2020; Canuto et al. 2018). As a consequence, hillshading of the noisy DTM computed below forest cover is also noisy and only the large structure can be observed without making too much of a visual effort (Figure 1). Furthermore, to process a good hillshade image would require to test several parameters of zscale and of sun angle for each LAS file, as depending on the sun angle parameter value some structures simply disappear (Figure 1e). The effective visualization of the geoglyphs in the hillshade image is highly dependent of the hillshade function parameters (Figure 2). Furthermore, finding good hillshade parameters for each individual LAS file would not be efficient for LiDAR datasets with several hundred or thousands of LAS files. The anomaly of elevation, at the exception of locations near pronounced inversion in elevation such as river, is not noisy and show smooth variation in contrast that make the detection very efficient and does not need to much visual effort. Finally, only looking at the colour of the anomaly of elevation, the user can directly determine if the geoglyph is outlined by a trench or a wall. Our method provides also a good normalized visualization for fast screening of geoglyphs when compared to the RVT toolbox main visualization functions with default parameters (Figure 3). Then, after detection, more details can be obtained only on the digital terrain model containing geoglyphs by the several tools provided by RVT Toolbox.

Currently, unprecedented amount of LiDAR data above tropical forests are collected in the Amazon and in other tropical forest regions (EBA 2016; Embrapa 2016; Fatoyinbo et al. 2021). For example, the Sustainable Landscapes Brazil project LiDAR dataset from which are extracted the two LAS files in Figure 1 is constituted of more than hundreds of LAS files above Brazilian tropical forests. There will be undoubtedly a growing need for fast assessment of archaeological structures with these large datasets, and our method could be applied to them for a fast detection and assessment of the pre-Colombian geoglyphs.

Acknowledgement

We thank the Sustainable Landscapes Brazil project supported by EMBRAPA, the US Forest Service, USAID and the US Department of State. Part of this work was carried out at the Jet Propulsion Laboratory, California Institute of Technology, under a contract with the National Aeronautics and Space Administration (NASA).

Disclosure statement

No potential conflict of interest was reported by the authors.

Funding

F.H.W. and R.D. have been funded by FAPESP (grant 2015/50484-0 and 2019/21662-8). V.P. was supported by CAPES (grant 88887.479608/2020-00).

ORCID

Ricardo Dalagnol http://orcid.org/0000-0002-7151-8697
Luiz E.O.C. Aragão http://orcid.org/0000-0002-4134-6708
Mayumi C. M. Hirye http://orcid.org/0000-0002-1817-360X

References

Bennett, R., K. Welham, R. A. Hill, and A. Ford. 2012. "A Comparison of Visualization Techniques for Models Created from Airborne Laser Scanned Data." *Archaeological Prospection* 19 (1): 41–48. doi:10.1002/arp.1414.

Canuto, M. A., F. Estrada-Belli, T. G. Garrison, S. D. Houston, M. J. Acuña, M. Kováč, D. Marken, et al. 2018. "Ancient Lowland Maya Complexity as Revealed by Airborne Laser Scanning of Northern Guatemala". *Science* 361: 6409. doi:10.1126/science.aau0137.

Challis, K., P. Forlin, and M. Kincey. 2011. "A Generic Toolkit for the Visualization of Archaeological Features on Airborne LiDar Elevation Data." *Archaeological Prospection* 18 (4): 279–289. doi:10.1002/arp.421.

Chase, A. F., D. Z. Chase, C. T. Fisher, S. J. Leisz, and J. F. Weishampel. 2012. "Geospatial Revolution and Remote Sensing LiDar in Mesoamerican Archaeology." *Proceedings of the National Academy of Sciences* 109 (32): 12916–12921. doi:10.1073/pnas.1205198109.

De Souza, J. G., M. Robinson, S. Y. Maezumi, J. Capriles, J. A. Hoggarth, U. Lombardo, V. F. Novello, et al. 2019. "Climate Change and Cultural Resilience in Late Pre-Columbian Amazonia." *Nature Ecology & Evolution* 3 (7): 1007–1017. doi:10.1038/s41559-019-0924-0.

Doneus, M., and C. Briese. 2006. "Full-Waveform Airborne Laser Scanning as a Tool for Archaeological Reconnaissance." *BAR International Series* 1568: 99.

EBA. 2016. "*Improving Biomass Estimation Methods for the Amazon*." Technical Report. http://www.ccst.inpe.br/projetos/eba-estimativa-de-biomassa-na-amazonia/.

Embrapa. 2016. "*Sustainable Landscapes Program*." Technical Report. https://www.paisagenslidar.cnptia.embrapa.br/webgis/.

Evans, D. H., R. J. Fletcher, C. Pottier, J.-B. Chevance, D. Soutif, B. S. Tan, S. Im, et al. 2013. "Uncovering Archaeological Landscapes at Angkor Using Lidar." *Proceedings of the National Academy of Sciences* 110 (31): 12595–12600. doi:10.1073/pnas.1306539110.

Fatoyinbo, T., J. Armston, M. Simard, S. Saatchi, M. Denbina, M. Lavalle, M. Hofton, et al. 2021. "The NASA AfriSar Campaign: Airborne SAR and Lidar Measurements of Tropical Forest Structure and Biomass in Support of Current and Future Space Missions". *Remote Sensing of Environment* 264: 112533. doi:10.1016/j.rse.2021.112533.

Fisher, C. T., A. S. Cohen, J. C. Fernández-Diaz, and S. J. Leisz. 2017. "The Application of Airborne Mapping LiDar for the Documentation of Ancient Cities and Regions in Tropical Regions." *Quaternary International* 448: 129–138. doi:10.1016/j.quaint.2016.08.050.

Henry, E. R., C. R. Shields, and T. R. Kidder. 2019. "Mapping the Adena-Hopewell Landscape in the Middle Ohio Valley, USA: Multi-Scalar Approaches to LiDar-Derived Imagery from Central Kentucky." *Journal of Archaeological Method and Theory* 26 (4): 1513–1555. doi:10.1007/s10816-019-09420-2.

Hesse, R. 2010. "LiDar-Derived Local Relief Models–a New Tool for Archaeological Prospection." *Archaeological Prospection* 17 (2): 67–72.

Iriarte, J., M. Robinson, J. G. de Souza, A. Damasceno, F. da Silva, F. Nakahara, A. Ranzi, and L. Aragao. 2020. "Geometry by Design: Contribution of Lidar to the Understanding of Settlement Patterns of the Mound Villages in SW Amazonia." *Journal of Computer Applications in Archaeology* 3 (1): 151–169. doi:10.5334/jcaa.45.

Khan, S., L. Aragão, and J. Iriarte. 2017. "A Uav–lidar System to Map Amazonian Rainforest and Its Ancient Landscape Transformations." *International Journal of Remote Sensing* 38 (8–10): 2313–2330. doi:10.1080/01431161.2017.1295486.

Kokalj, Ž., and M. Somrak. 2019. “Why Not a Single Image? Combining Visualizations to Facilitate Fieldwork and On-Screen Mapping.” *Remote Sensing* 11 (7): 747. doi:10.3390/rs11070747.

Kokalj, Ž., K. Zakšek, and K. Oštir. 2011. “Application of Sky-View Factor for the Visualisation of Historic Landscape Features in Lidar-Derived Relief Models.” *Antiquity* 85 (327): 263–273. doi:10.1017/S0003598X00067594.

Mann, C. C. 2008. “Ancient Earthmovers of the Amazon.” *Science* 321 (5893): 1148–1152. doi:10.1126/science.321.5893.1148.

Mestre, M., G. Vincent, C. Bedeau, N. Antonoff, O. Brunaux, P. Gautreau, and M. Noucher. 2020. “Detecting Ditched Sites on Lidar-Generated Digital Elevation Models: From Technical Specifications to Interpretation Keys. In Odonne, Guillaume, Molino, Jean-François (eds), *Methods in Historical Ecology*, 68–75. Milton Park: Routledge.

Morgan-Wall, T. 2020. “Rayshader: Create Maps and Visualize Data in 2D and 3D.” https://github.com/tylermorganwall/rayshader.

R Core Team. 2020. *R: A Language and Environment for Statistical Computing*. Vienna, Austria: R Foundation for Statistical Computing. https://www.R-project.org/.

Roussel, J.-R., and D. Auty. 2020. “Airborne LiDar Data Manipulation and Visualization for Forestry Applications.” https://cran.r-project.org/package=lidR.

Stenborg, P., D. P. Schaan, and C. G. Figueiredo. 2018. “Contours of the Past: LiDar Data Expands the Limits of Late Pre-Columbian Human Settlement in the Santarém Region, Lower Amazon.” *Journal of Field Archaeology* 43 (1): 44–57. doi:10.1080/00934690.2017.1417198.

Watling, J., J. Iriarte, F. E. Mayle, D. Schaan, L. C. R. Pessenda, N. J. Loader, F. A. Street-Perrott, R. E. Dickau, A. Damasceno, and A. Ranzi. 2017. “Impact of Pre-Columbian “Geoglyph” Builders on Amazonian Forests.” *Pnas* 114 (8): 1868–1873. doi:10.1073/pnas.1614359114.

Zakšek, K., K. Oštir, and Ž. Kokalj. 2011. “Sky-View Factor as a Relief Visualization Technique.” *Remote Sensing* 3 (2): 398–415. doi:10.3390/rs3020398.